

Pierluigi Reschiglian<sup>a)</sup>,  
Barbara Roda<sup>a)</sup>,  
Andrea Zattoni<sup>a)</sup>,  
Byung Ryul Min<sup>b)</sup>,  
Myeong Hee Moon<sup>c)</sup>

## High performance, disposable hollow fiber flow field-flow fractionation for bacteria and cells. First application to deactivated *Vibrio cholerae*\*

<sup>a)</sup> Department of Chemistry  
“G. Ciamician”, Via Selmi 2,  
I-40126 Bologna, Italy

<sup>b)</sup> Department of Chemical  
Engineering, Yonsei University,  
Seoul 120–749, Korea

<sup>c)</sup> Department of Chemistry,  
Pusan National University,  
Pusan 609–735, Korea

Interest in low-cost, analytical-scale, highly efficient, and sensitive separation methods for cells and bacteria has recently been increasing. Field-flow fractionation is well suited to the separation of different types of cells, including bacteria. High performance hollow fiber flow field-flow fractionation of such samples is demonstrated here for the first time with potentially disposable channels and high-sensitivity UV/Vis detectors. In this first application, hollow fiber flow field-flow fractionation is used to fractionate bacteria of biotechnological interest such as deactivated *Vibrio cholerae*, which are employed for whole-bacteria vaccine production. Quite short analysis times, high reproducibility, and low limits of detection are found. Retention of *Vibrio cholerae* is shown to depend on the mobile phase composition. Two serologically different *Vibrio cholerae* strains are partly distinguished by their fractogram profiles.

**Key Words:** Hollow fiber flow field-flow fractionation; HF FIFFF; Cell separation; Whole-bacteria vaccines; *Vibrio cholerae*

Received: October 29, 2001; revised: February 8, 2002; accepted: February 11, 2002

### 1 Introduction

The term field-flow fractionation (FFF) refers to a family of separation techniques able to fractionate, either on an analytical or on a micro-preparative scale for further characterization, a broad range of macromolecular, nano- and micro-sized particles, of either inorganic or biological origin [1]. Among the FFF techniques, flow FFF (FIFFF) shows the highest separation versatility. Classical FIFFF separators have a flat channel design, with the ribbon-like channel cut out from a thin plastic foil (spacer) with a rectangular profile and tapered ends. FIFFF employs a secondary, transverse flow as the external field. The spacer is thus sandwiched between two plastic walls into which permeable frits are inserted, either on both sides (symmetrical FIFFF [2]) or on only one side (asymmetrical FIFFF [3]). Both these configurations are available in commercial FIFFF separators. Other than to the classical rectangular design, the idea of using hollow fiber (HF) membranes as cylindrical channels for FIFFF was reported as early as 1974 [4]. HF feasibility for FIFFF was first described in few

papers in which HF FIFFF was shown able to separate polystyrene latex standards [5–10]. Investigations were reported on the effects of carrier ionic strength [7], membrane properties [9], and sample overloading [10] on HF FIFFF retention. Further attempts were made to separate a few proteins and water-soluble polymers [11, 12] and, most recently, synthetic organic-soluble polymers [13]. However, particle separation in HF FIFFF has only recently been improved to an efficiency level normally achieved by conventional, rectangular FIFFF channels [14]. These improvements have been achieved through optimization of the HF FIFFF channel design and relevant instrumental system. With these HF FIFFF systems an increase in separation speed and resolution of nano-sized particles has been accomplished and, by increasing the working temperature, with extension to a size range as high as 1  $\mu\text{m}$  [15]. Even though HF FIFFF can be considered as still being in its early development stage, its potential for effecting particle separation at low cost and low sample loads has already been demonstrated. Elution in HF FIFFF follows the basic principles of FIFFF, except that separation takes place in a cylindrical fiber instead of a rectangular channel. In HF FIFFF, retention times in normal mode are directly proportional to the diffusion coefficient ( $D$ ) of the analyte, and inversely proportional to the HF radius ( $r_f$ ). For highly retained analytes, the retention ratio was expressed as [14–15]

$$R = \frac{t_0}{t_r} \cong \frac{4D}{Ur_f} \quad (1)$$

**Correspondence:** Pierluigi Reschiglian, Department of Chemistry “G. Ciamician”, Via Selmi 2, I-40126 Bologna, Italy.

**E-mail:** resky@ciam.unibo.it

**Fax:** +39 051 2099456

\* Work presented at FFF 2001, 19<sup>th</sup> International Symposium on Field-Flow Fractionation, Golden, Colorado, USA, June 26–29, 2001.

where  $t_0$  is the void time,  $t_r$  the retention time, and  $U$  the radial flow velocity at the fiber wall.

The key advantage of this latest version of HF FIFFF lies in its instrumental simplicity, low-cost, and miniaturization. These features offer potential for disposable usage. Disposable separators can be particularly appealing for analytical and micro-preparative scale bio-separations, for which either sterility or inter-run reproducibility are critical. In these cases, the risk of sample contamination and inter-run memory effects constitutes a serious drawback. This is particularly true for complex samples like bacterial or other living cells.

Analysis of bacteria by separation methods is of great interest since bacteria are used in such diverse fields as biomedical applications, biotechnology, and, unfortunately, biological warfare. When present in complex samples (e.g. foodstuffs, blood, or environmental matrices), bacteria, which can be highly dangerous or lethal even in low numbers, can actually be difficult to isolate from other particles and to quantitate. Separation of bacteria prior to detection and identification can thus minimize interference and provide more reliable results. Also the ability to distinguish live or dead bacteria is important. For instance, pathogenicity is usually a property of living bacteria and the antibiotic effect of drugs is directly related to their killing activity. On the other hand, deactivated (dead) bacteria are of biotechnological interest for whole-bacteria vaccines. These vaccines are designed to elicit an antibody response through the bacterial membrane surface features that effect the immuno-response to the bacteria-associated antigens. Culturing, haemo-agglutination, and ELISA are among the classical methods for differentiating live and dead bacteria, and for establishing the immuno-response of deactivated bacteria. However, they are not separation techniques and analyses are time consuming.

It is not thus surprising that interest in low-cost, high-efficiency separation methods for bacteria analysis is rapidly increasing. FFF has already proved to be well suited for separation, on an analytical scale, of different type of cells [16], including bacteria [17]. In this work it is shown for the first time that HF FIFFF can be used to fractionate bacterial cells at low cost and with a performance comparable to that of classical FFF channels. HF FIFFF is here applied to deactivated *Vibrio cholerae* (*V. cholerae*). The most common classification given by Sakazaki and Shimada recognizes 139 serogroups for *V. cholerae* [18]. Cholera epidemics are usually caused by the O1 serogroup, which forms part of the lipo-polysaccharide overall content in the bacterial outer membrane. This O1 serogroup is further divided into subgroups, the most interesting of which for vaccine productions are *Inaba* and *Ogawa*. Deactivated *V. cholerae* are sub-micron sized, rod-shaped bacteria with a non-motile tail. Motility is indeed lost when bacteria

are deactivated. It is shown here that it is possible to obtain high performance HF FIFFF of *V. cholerae* at quite short analysis time and high reproducibility. Retention of *V. cholerae* was found to be dependent on the mobile phase composition. The two serologically different *V. cholerae* strains *Inaba* and *Ogawa* were partly distinguished by their elution profiles. This is most likely a consequence of the different lipo-polysaccharide contents of the bacterial membrane. The use of a coupled, high-sensitivity diode-array UV/Vis detector (UV/DAD) equipped with a fiber optic guide (FO) light-pipe cell allowed for HF FIFFF at a low detection limit. This HF FIFFF-FO/UV/DAD system was thus shown to be suited for separating and further identifying a low number of *V. cholerae* in liquid dispersion.

## 2 Materials and methods

### 2.1 HF FIFFF system

The HF channel was built up as previously described [14, 15], except that the 1/8" tee union inserted for the radial flow rate outlet was here in nylon. The hollow fiber used was made of polysulfone, having a molecular weight cut-off of 30,000 Da, supplied by SK Chemicals (Seoul, Korea). The dimensions of the fiber were 24.0 cm in length ( $L$ ) and 0.040 cm in nominal, inner radius ( $r_i$ ) (dry conditions). The mobile phase was delivered by a model 422 A HPLC pump (Bio-Tek-Kontron Instruments, Milan, Italy). An FO/UV/DAD model UV 6000 LP (ThermoQuest, Austin, TX) was employed.

### 2.2 Mobile phases and samples

Carrier solutions were prepared from ultrapure water (MilliQ Simplicity, Millipore, Bedford, MA). The buffer PBS 0.150 M and the well-known solution for particle separation in FFF (FL-70/NaN<sub>3</sub>) were used. FL-70 (Fisher Scientific Co., Fair Lawn, NJ) was added to water at 0.1%  $v/v$  and NaN<sub>3</sub> at a concentration varying from  $3 \times 10^{-4}$  to  $3 \times 10^{-2}$  M. Two samples of deactivated *V. cholerae* from whole-bacteria vaccine production were supplied by SBL Vaccin AB (Solna, Sweden). Each sample corresponded to the pure serotype *Inaba* (strain KIH1797) and *Ogawa* (strain KOH1597), originally suspended in 9.5 mM PBS, pH 7.4. For both strains, batch concentrations were comparable and of the order of  $10^{11}$  cells/mL. The lipo-polysaccharide content of the bacterial surface was determined by enzyme-linked immunosorbent assay (ELISA) and corresponded to 700 EU/mL for *Inaba* and 1151 EU/mL for *Ogawa*. Before injection samples were diluted in the relevant mobile phase to an approximate concentration of  $10^9$  cells/mL.

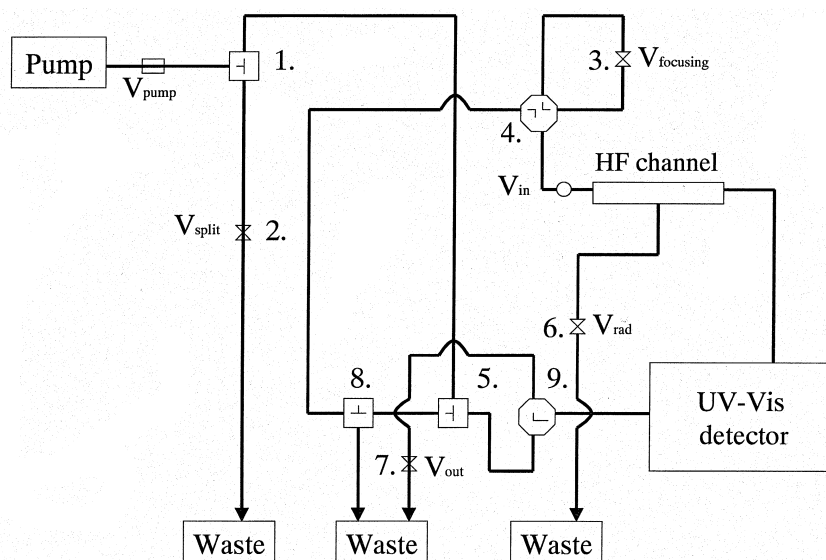


Figure 1. Scheme of the HF FIFFF system.

### 2.3 HF FIFFF configuration and operations

For this work the HF FIFFF system configuration already reported in early work [14, 15] was modified as shown in **Figure 1**. The new scheme was proposed to employ a single pump set at a constant flow rate value during all analysis steps. The complete run cycle constituted four steps, each step corresponding to different flow rates and flow patterns: a) injection, b) focusing/relaxation, c) elution, d) flow-feedback. During all the analysis steps a)–c) the pump flow rate was set at a constant value ( $V_{\text{pump}} = 1.52 \text{ mL/min}$ ), while for the final step d) it was increased manually. Sample injection was performed via a Model 7125 injection valve (Rheodyne, Cotati, CA) equipped with an external loop of  $5.0 \mu\text{L}$ . Flow rates at all waste outlets ( $V_{\text{split}}$ ,  $V_{\text{rad}}$ ,  $V_{\text{out}}$ , Figure 1) were adjusted with the aid of SS-SS2-VH Nupro metering valves (Nupro, Willoughby, OH) (valve 2, 6, 7, Figure 1), with flow rate values measured by burettes and chronometer. Before the injection, the flow injection rate was reduced to  $0.43 \text{ mL/min}$  by splitting constant  $V_{\text{pump}}$  via a 3-way, tee valve (Hamilton, Reno, NV) (valve 1, Figure 1) and by adjusting valve 2. After sample injection, the focusing/relaxation process was carried out at the same  $V_{\text{pump}}$  value, by further splitting the  $V_{\text{in}}$  flow into two parts (delivered to both inlet and outlet of the HF channel) via a 3-way, tee valve (Hamilton) (valve 5, Figure 1) and a 2-way, “L” valve (Upchurch, Oak Harbor, WA) (valve 9, Figure 1). The sample focusing position was dependent on the chosen flow ratio, which was set by switching a 4-way, diagonal flow valve (Upchurch) (valve 4, Figure 1) and adjusted with an additional fine metering Nupro valve ( $V_{\text{focusing}}$ , valve 3, Figure 1). The focusing position was determined using HF FIFFF retention theory [14], by measuring the retention and resolution of a mixture of

two polystyrene (PS) latex standards, having nominal diameters  $0.050 \mu\text{m}$  and  $0.155 \mu\text{m}$  (Duke Scientific Co. Palo Alto, CA). The focusing time was in the range of 2 to 3 min. The elution flow pattern was set by switching valves 4, 5, and 9, while switching valve 1 makes all  $V_{\text{pump}}$  flow stream be fed to the HF channel inlet ( $V_{\text{in}}$ ). The required radial ( $V_{\text{rad}}$ ) and axial ( $V_{\text{out}}$ ) flow rate values were pre-set by adjusting valve 6 and 7. The flow-feedback step was set when the sample elution was finished. For flow-feedback,  $V_{\text{pump}}$  was increased to a value of  $6.0 \text{ mL/min}$  and flow pattern then reversed for at least 1 min from the detector outlet to the HF channel inlet, by acting on valve 5 and 9 and on the additional 3-way, tee switching valve (Hamilton) (valve 8, Figure 1). This caused the detector cell, the HF channel, and the injection loop be back-flushed at a high flow rate and without any field ( $V_{\text{rad}} = 0$ ) for system clean-up before the next run.

### 2.4 Quasi-elastic light scattering for sizing

Size analysis of *V. cholerae* strains in different dispersing media was performed by quasi-elastic light scattering (QELS) using a 90Plus Particle Sizer (Brookhaven Instruments Corporation, Holtsville, NY, USA). Before analysis, batch samples were diluted 1:1000 in the relevant dispersing medium to a concentration of about  $10^8 \text{ cells/mL}$ , and then allowed to equilibrate for at least 15 min. The sample holder was a quartz, 1-cm path length cuvette for spectrofluorimetry. The incident radiation was set at  $532.0 \text{ nm}$  wavelength. The scattered light was read at  $90^\circ$  from the direction of the incident beam. The instrument software (90Plus Particle Sizing Software Ver. 2.31) gave the values of sample effective diameter, half width of the size

distribution and polydispersity, all expressed as mean values from three runs of two minutes each. Sample temperature was kept constant at 37.0°C, and a viscosity of 0.692 cP was assumed for all samples. A software dust filter for particles larger than 10 µm was employed in all cases.

### 3 Results and discussion

#### 3.1 System calibration

The HF FIFFF system required a preliminary calibration before application to *V. cholerae*. The most important parameters to be determined were the focusing position and the fiber inner radius. They respectively define the actual length and thickness of the separation channel. The focusing/relaxation of the injected sample components is usually accomplished inside the channel at position 0.1  $L$  from the inlet (where  $L$  is the geometrical length of the fiber) [14, 15]. However, with respect to asymmetrical FIFFF with rectangular channel design and transparent depletion wall in which a dye is used to find the focusing position [3], in HF FIFFF we have found no means to visualize focalization. The best focalization point was thus found by first pre-setting, via the relevant metering valves, the flow ratio inside the channel, from the inlet to the outlet and from the outlet to the inlet, at about 1:9, as reported in literature [14, 15]. Subsequently, the correct focusing position was tested by the evaluation of the highest retention and resolution between two PS standards (see Section 2: Materials and Methods). The higher resolution and the higher retention times, the closer the focalization distance from the channel inlet. For the experiments,  $V_{in} = 1.41$  mL/min,  $V_{rad} = 0.10$  mL/min.

The value of the actual inner fiber radius  $r_f$  is to be measured because of its already observed dependence on channel flow rate. This dependence was explained as the result of fiber expansion caused by the system pressure [14]. The actual  $r_f$  value was calibrated using HF FIFFF retention theory [14] by measuring the experimental diffusion coefficient ( $D$ ) of a standard protein (horse spleen ferritin, from Sigma-Aldrich Chemie, Steinheim, Germany) under different flow rate conditions. The resulting  $r_f$  value was  $0.051 \pm 0.001$  cm, which was found to be independent of flow rate ( $V_{in} = 1.13$ – $2.19$  mL/min). This comparatively constant value can be explained by the very low pressure (less than 70 kPa) that builds up in the HF FIFFF-FO/UV/DAD system described here. Compared to previously presented HF FIFFF systems, which employed UV/Vis detectors with standard cells [14, 15], the use of a light-pipe detector cell with negligible back-pressure was mainly responsible for the low system pressure found here.

#### 3.2 HF FIFFF of *V. cholerae*: limit of detection and reproducibility

The advantages of using a light-pipe detector cell in HF FIFFF operations are not limited to its low back-pressure but also include increased detection sensitivity. Actually, the nominal path-length ( $b$ ) of the detector cell employed here was five-fold longer than in the case of standard UV/Vis detectors for HPLC, which are usually equipped with “Z”-duct, analytical cells ( $b \leq 1$  cm). The real cell path-length of the light-pipe detector cell was experimentally determined as described in the literature [19] by calibration with solutions at different concentration of a spectroscopic standard of known molar absorptivity ( $K_2CrO_4$  in  $Na_2HPO_4$  0.05 M;  $\epsilon = 4.82 \times 10^6$  cm<sup>2</sup> mol<sup>-1</sup> at  $\lambda = 373$  nm). It was found to be  $b = 4.6 \pm 0.3$  cm. According to the Beer-Lambert-like law for quantitative analysis of dispersed samples by UV/Vis spectroscopy [19–21], one might thus expect a corresponding improvement in analytical sensitivity and limit of detection. In fact, the limit of detection is expected to further diminish because of the high signal-to-noise ratio values due to the reduced dispersion of light intensity through the optics of such fiber optic guide detectors. Evaluation of the limit of detection for the HF FIFFF-FO/UV/DAD system described in this work was first performed with standard PS particles. Different and known amounts of PS 155 nm were analyzed and peak area measured. Regression analysis gave: Area [ $\mu$ AU min] =  $(330 \pm 17)$  mass [ng] +  $(3600 \pm 600)$  ( $N = 16$ ). This corresponded to a limit of detection for PS of 7.4 ng. The mass of PS particles that corresponds to this limit of detection is one order of magnitude lower than the amount of PS injected in previous works employing these HF FIFFF channels fed to conventional UV/Vis detectors [14, 15]. For the injection of *V. cholerae* a limit of detection of approximately 500,000 cells was then found, which is competitive with the lowest number of bacterial cells able to be counted by classical methods for bacteria counting as well as cultivation.

Reproducibility was one of the major concerns in early HF FIFFF. In **Figure 2** are superimposed some HF FIFFF fractograms of the two strains (*Inaba*, *Ogawa*) obtained from different, successive runs under the same experimental conditions. Fractograms of each strain in Figure 2 appear quite reproducible within runs, and show no significant differences with use. Good inter-run reproducibility was always observed. In order to show reproducibility, here and in all the Figures discussed in further sections, for each experiment the fractograms obtained in subsequent runs are superimposed. Prominent void peaks were always observed. These were actually transient peaks, originated from valve switching before the elution step and after the focusing/relaxation step. The light-pipe DAD employed in this work is, in fact, particularly sensitive to changes in flow direction and intensity. The absence of

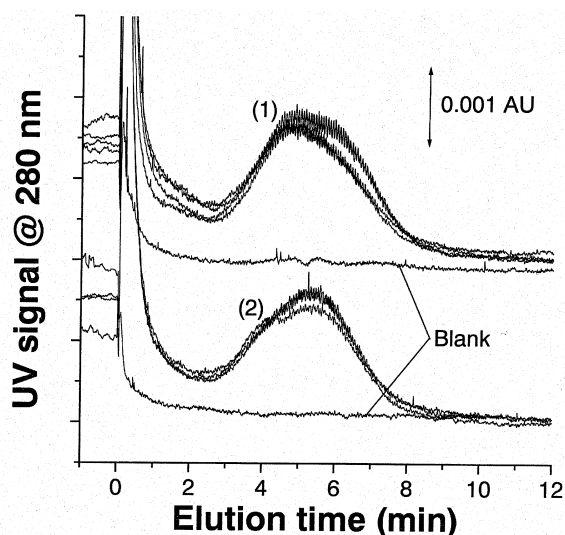


**Figure 2.** Reproducibility of HF FIFFF of *V. cholerae*. Serotypes: *Inaba* (1, four repeated runs), *Ogawa* (2, three repeated runs); injected cells ca.  $5 \times 10^6$  (in  $5 \mu\text{L}$ ); mobile phase: PBS 150 mM;  $V_{in} = 1.5 \text{ mL/min}$ ,  $V_{rad} = 0.038 \text{ mL/min}$ .

bacteria aggregation was confirmed by PCS measurements on the samples (see Table 1, below). Otherwise, the focusing/relaxation process was optimized, as reported in Section 2.

Figure 2 also shows no inter-run memory effects, as we could see from the blanks performed after *V. cholerae* runs. A single HF FIFFF channel is thus exploitable for reproducible, multiple runs of even complex biological samples. However, it must be noted that, at the rather low field strength condition first employed ( $V_{rad} = 0.38 \text{ mL/min}$ ) the two serotypes cannot be distinguished by the fractogram profiles.

### 3.3 *Inaba* and *Ogawa* size distribution

In FIFFF, retention ideally depends only on sample size. Therefore, in order to find the best flow conditions and to ascertain whether the two *V. cholerae* strains can be resolved by HF FIFFF, the most fundamental sample feature to be measured by an uncorrelated technique is size. Since *V. cholerae* is not spherical, the definition of its size is not trivial. In most real cases of irregular particles, however, the size can be usually expressed in terms of a sphere equivalent to the particle with regard to some of its

properties [22]. The hydrodynamic radius can thus be taken as an estimation of the size of irregular particles. Quasi-elastic light scattering (QELS) (otherwise called photon correlation spectroscopy; PCS) is a well-established technique for measuring the hydrodynamic radius of submicron sized particles [23]. Table 1 lists the hydrodynamic radii determined by QELS for the serotypes *Inaba* and *Ogawa*. It is first to be noted that the small size of *V. cholerae* precludes size measurements by either flow cytometry or Coulter counter.

Samples were suspended in the different mobile phases in order to determine whether the mobile phase composition could affect size. From these data we can observe differences in size either when any strain is suspended in mobile phases of different compositions or when the two strains are compared in a given mobile phase. Although the error margins given in Table 1 suggest that, in any case, differences in size might not be highly significant, one can deduce that changing mobile phase composition and increasing radial flow rate might help in resolving the two serotypes. This is, first of all, because size resolution in FIFFF increases with increasing field strength. Secondly, osmolarity effects on cell size are known to influence FFF retention [24–25]. Thirdly, differences in membrane composition (i.e. the lipo-polysaccharide content) between the two strains could induce changes in some bacterial cell indices that might be sensitive to the mobile phase composition (e.g. the presence of surfactant).

However, the most important point to notice in Table 1 is that the average sizes of both strains lie around the transition point between normal and steric/hyperlayer mode, which had been previously determined with PS latex standards and identical HF FIFFF channels [15]. The particle size at which the transition occurs in HF FIFFF was shown to depend on the instrumental and experimental conditions under which samples are eluted. In order to evaluate the transition point one might take into account, in contrast to retention in the normal mode [Eq. (1)], the complete expression that holds true around the transition region [15]

$$R \cong \frac{4kT}{3\pi\eta U r_f d} + \frac{t_0}{t_{r1}} d^S \quad (2)$$

where  $\eta$  is the mobile phase viscosity,  $t_{r1}$  the retention time of a particle of unit diameter, and  $S$  the experimental,

**Table 1.** QELS measurements on *V. cholerae* strains.

Serotype	<i>Ogawa</i>				<i>Inaba</i>	
	FL-70 / $\text{NaN}_3$	PBS	PBS / FL-70	FL-70 / $\text{NaN}_3$	PBS	PBS / FL-70
Carrier	FL-70 / $\text{NaN}_3$	PBS	PBS / FL-70	FL-70 / $\text{NaN}_3$	PBS	PBS / FL-70
Effective diameter (nm)	$474.5 \pm 6.2$	$532.1 \pm 24.6$	$692.3 \pm 30.5$	$356.9 \pm 26.6$	$646.0 \pm 28.7$	$577.0 \pm 35.2$
Half width (nm)	$257.6 \pm 9.8$	$296.7 \pm 28.9$	$388.2 \pm 60.6$	$186.3 \pm 11.8$	$345.1 \pm 26.0$	$362.0 \pm 51.6$
Polydispersity	0.295	0.311	0.387	0.272	0.285	0.394

size-based selectivity. Differentiation of the above expression finally gives the value of the diameter at which the transition between normal and steric/hyperlayer HF FIFFF mode occurs ( $d_i$ ), that is the point at which  $\partial R/\partial d = 0$

$$d_i = \left( \frac{4kt_{r1}}{3\pi r_f U S t_0} \frac{T}{\eta} \right)^{1/(1+S)} \quad (3)$$

Since in asymmetrical, steric/hyperlayer FIFFF with rectangular channel design the experimental, absolute value of  $S$  was recently found above unity ( $1 < |S| \leq 1.3$ , [26]), from the above expression it can be confirmed that for our HF FIFFF channels under similar experimental conditions (i.e. radial flow rates, room temperature, and aqueous mobile phases) the transition point can be found at a particle diameter as low as  $0.5 \mu\text{m}$  [15]. However, it must be noted that the above  $S$  values were determined using standard, rigid PS beads. In fact, the elution behavior of non-spherical, non-rigid particles in steric/hyperlayer mode is known to be markedly different from that of rigid spheres. Most recently, selectivity in steric/hyperlayer, asymmetrical, parallel plate FIFFF of rod-shaped *Escherichia coli* has been observed to be different from that on PS beads, and to be dependent on differences in flexibility originating from differences in bacterial surface features [27]. However, a systematic approach to the retention mechanism of *V. cholerae* in HF FIFFF lies beyond the scope of the present work. From the above definition of  $d_i$ , the retention ratio at the transition region in HF FIFFF is independent of size, as generally known for FFF. As a consequence, one might expect to neither easily distinguish the two serotypes nor correlate their size with retention.

### 3.3.1 Effects of mobile phase composition

Although not particularly significant, the size differences between *Inaba* and *Ogawa* obtained by QELS (Table 1) when any strain was suspended in different mobile phases suggested, as mentioned above, an active role of the mobile phase composition in retention of *V. cholerae*. Particularly, because of the difference in lipo-polysaccharide content in the cell membrane composition between *Inaba* and *Ogawa*, any surfactant present could be expected to differently modify bacterial surface properties, thus leading to differences in retention. As a consequence, in order to increase differences in HF FIFFF profiles between the two strains, mobile phase composition was modified by changing the salt concentration and the presence of surfactant. **Figure 3** shows repeated fractograms for the *Ogawa* strain obtained with PBS 150 mM with surfactant. Analysis conditions were the same as in Figure 2. Comparison of Figure 2, case (2) and Figure 3 reveals that in the presence of surfactant retention was greatly reduced and signals increased by one order of magnitude. Such an increase can be observed in both the

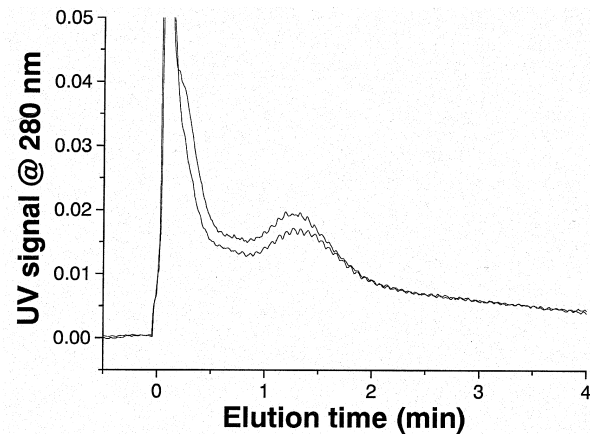


**Figure 3.** Effect of mobile phase composition on HF FIFFF of *V. cholerae*: presence of surfactant. Serotype: *Ogawa*; injected cells ca.  $5 \times 10^6$  (in  $5 \mu\text{L}$ );  $V_{in} = 1.5 \text{ mL/min}$ ,  $V_{rad} = 0.038 \text{ mL/min}$ ; mobile phase: FL-70 0.1% v/v/PBS 150 mM, two repeated runs.

void and the sample peak. This can be explained by the influence of surfactants on extinction coefficients with UV/Vis turbidity detection [21]. The large reduction in retention cannot be explained in terms of a corresponding reduction in size, according to HF FIFFF retention theory [14]. In fact, data in Table 1 would rather indicate an increase in *Ogawa* size when surfactant is added to PBS. It is known, however, that in FFF a reduction of particle-particle or particle-wall attractive effects can be ascribed to the presence of surfactant in mobile phases of high ionic strength [28]. It is also possible that surfactant could be able to modify flexibility of the bacterial membrane or tail, which can consequently modify retention. **Figure 4.a–b** depicts the effect on HF FIFFF profiles of a drastic reduction in salt concentration in the mobile phase. Comparison of Figure 4.a–b with Figure 3 shows that a reduction in salt concentration from 0.150 M (in PBS, Figure 3) to 3.2 mM (in  $\text{NaN}_3$ , Figure 4.b) induces a slight, though reproducible increase in retention. This could be explained in terms of osmolarity effects on cell size. It is known that, with hypotonic dispersing media, cells tend to swell and FFF retention in normal mode tends to increase accordingly [24–25]. The mixed normal-steric/hyperlayer elution mode under which *V. cholerae* most likely elute tends to cancel such an effect on retention. However, a systematic optimization of the mobile phase composition for HF FIFFF of deactivated *V. cholerae* lies beyond the scope of this paper.

### 3.3.2 Effects of radial flow rate

In Figure 4 the two strains *Inaba* and *Ogawa* can be distinguished because of their different fractogram profiles. With respect to Figure 2, where the two strains do not show differences in retention, the fractograms in Figure 4

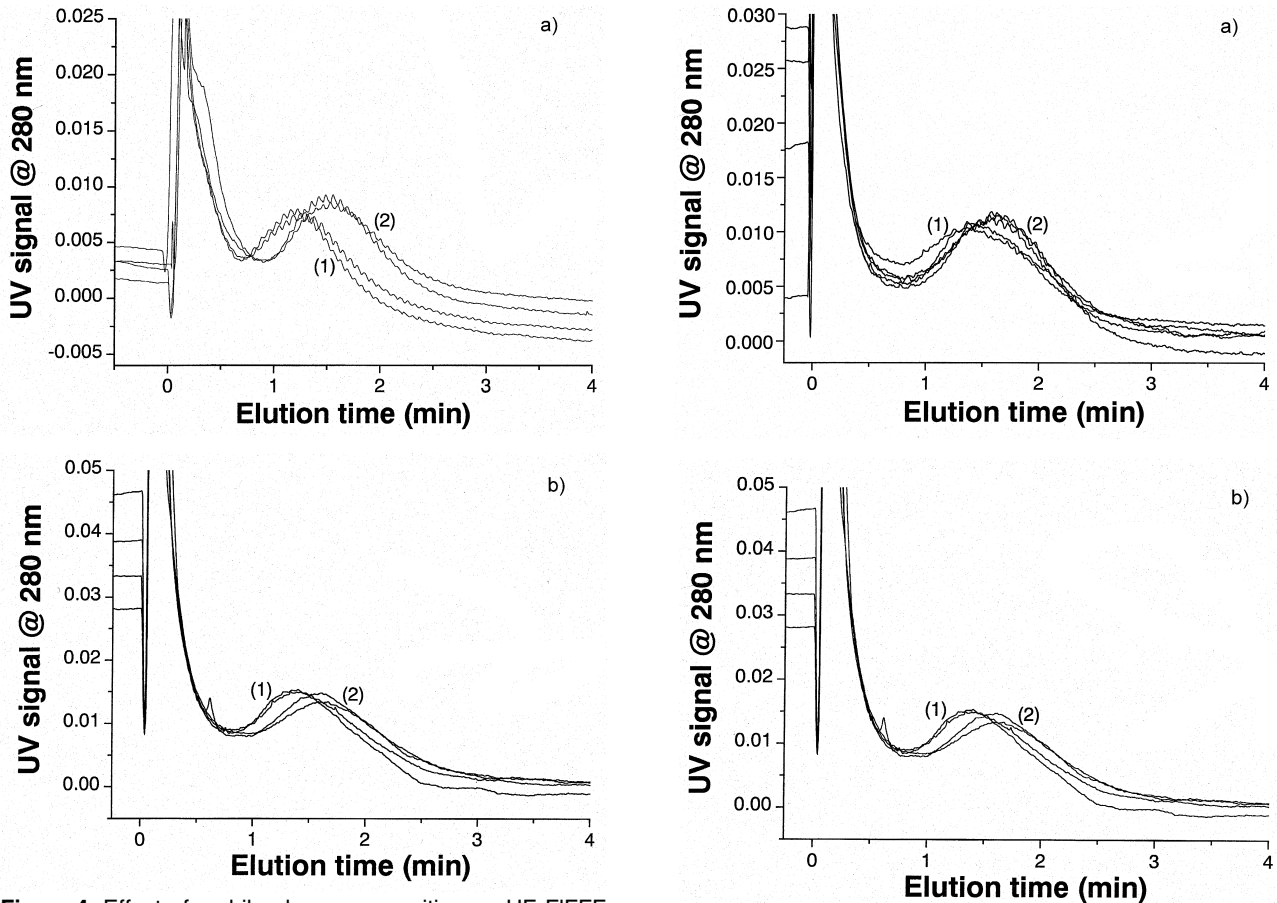


**Figure 4.** Effect of mobile phase composition on HF FIFFF of *V. cholerae*: different salt concentration. Serotypes: *Inaba* (1), *Ogawa* (2); injected cells ca.  $5 \times 10^6$  (in  $5 \mu\text{L}$ );  $V_{in} = 1.5 \text{ mL/min}$ ,  $V_{rad} = 0.051 \text{ mL/min}$ . a) FL-70 0.1% v/v/  $\text{NaN}_3$  32 mM, two repeated runs for (1) and (2); b) FL-70 0.1% v/v/ $\text{NaN}_3$  3.2 mM, two repeated runs for (1) and (2).

were, in fact, performed at higher radial flow rate ( $V_{rad} = 0.051 \text{ mL/min}$ , Figure 4;  $V_{rad} = 0.038 \text{ mL/min}$ , Figure 2). This would indicate that an increase of the applied field is able to increase differences in retention between *Inaba* and *Ogawa*. The effect of a further increase in the radial flow rate (that is, the field) is reported in Figure 5.a–c. For this study it was used the mobile phase FL-70 0.1% and  $\text{NaN}_3$  3.2 mM. This mobile phase composition gave the highest differences in retention between *Inaba* and *Ogawa* (see Figure 4.b). In Figure 5.a–c one can in fact observe that retention and resolution between the two serotypes first remain constant and, then, tend to decrease with increasing field strength. This finding is only apparently contradictory since it could be explained in terms of a reduction in selectivity across the transition point between normal and steric/hyperlayer elution mode. Otherwise, if we compare in Figure 5.c the fractograms of *V. cholerae* with the fractogram of a mixture of three PS latex standards of smaller size, one can observe that

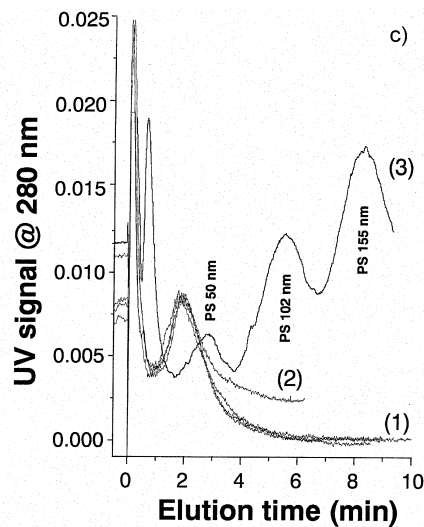


**Figure 5.** Effect of field strength on HF FIFFF of *V. cholerae*. Serotypes: *Inaba* (1), *Ogawa* (2); injected cells ca.  $5 \times 10^6$  (in  $5 \mu\text{L}$ ); mobile phase: FL-70 0.1% v/v/ $\text{NaN}_3$  3.2 mM;  $V_{in} = 1.5 \text{ mL/min}$ . a)  $V_{rad} = 0.042 \text{ mL/min}$ , two repeated runs for (1) and three repeated runs for (2); b)  $V_{rad} = 0.051 \text{ mL/min}$ , two repeated runs for (1) and (2); c)  $V_{rad} = 0.075 \text{ mL/min}$ , two repeated runs for (1) and (2); (3): HF FIFFF of a mixture of three PS latex standards, 50, 102, 155 nm diameter.

retention of both strains (1,2) is much lower than that of spherical particles of even smaller size, eluted under same conditions (3). This indicates that in HF FIFFF shape effects are also able to play an effective role in the retention of *V. cholerae*.

## 4 Conclusions

In this work it has been demonstrated for the first time that HF FIFFF is suited to the fractionation of submicron sized bacteria. With a separation performance comparable to that reported in the literature for conventional FIFFF of micron-size bacteria, HF FIFFF appears to be more convenient for several reasons. First, the cost of the HF FIFFF channels is very low, even in comparison with a single membrane for conventional FIFFF. Secondly, even though HF FIFFF proved to be quite reproducible within multiple runs, low cost and simplicity potentially allow for single-run, disposable usage. In fact, the risk of contamination and inter-run memory effects constitutes a serious drawback in membranes for conventional FIFFF, so much so that a membraneless approach has already shown some key advantages [29].

Two serotypes of *V. cholerae*, which differ in their lipopolysaccharide membrane content, have been only partly distinguished by HF FIFFF. This could be likely due to the lack of selectivity at the transition point between normal and steric/hyperlayer mode, the point around which *V. cholerae* most likely elute under the experimental conditions employed here. Work on determining the elution mechanism and hence on finding the optimized experimental conditions for HF FIFFF of *V. cholerae* is in progress.

In terms of instrumental advances, we have shown that a fiber optic guide, light-pipe detector cell is very suitable for our HF FIFFF channels. It improves not only sensitivity and limit of detection but also performance and reproducibility, because of better control of fiber deformation during use. Otherwise, the use of DAD for single-run, experimental evaluation of particle optical properties in flow-assisted separation systems has recently been described [30]. HF FIFFF-FO/UV/DAD should thus be able not only to separate but also to count cells or bacteria. HF FIFFF-FO/UV/DAD of bacteria and cells will be the object of further papers since our HF FIFFF channels have been recently applied also to micron-size particles [31].

We see great potential for the application of HF FIFFF-FO/UV/DAD to the fractionation of different type of live bacteria or cells (cell sorting), because of the simplicity of the method, the potentially disposable mode of use, and the quantitative response provided by single-run analysis.

## Acknowledgments

Hollow fibers were kindly supplied by SK Chemicals, Seoul. K. Rodmalm and E. Whitmore-Carlsson, SBL Vaccin AB, are duly acknowledged for accurate details on sample specifications and helpful discussions. Thanks also go to M. Guardigli, Department of Pharmaceutical Science, University of Bologna, for QELS measurements, and to S. Casolari and L. Cinque, Department of Chemistry "G. Ciamician", for technical assistance and practical work with the HF FIFFF systems.

## Grants

Work partially supported by Leonardo-EXCHANGE 2001 between the University of Bologna, (Italy) and SBL Vaccin AB, Solna (Sweden), financial program for researcher mobility from university to small and medium enterprises within the EU.

## References

- [1] J.C. Giddings, *Science* **1993**, *260*, 1456.
- [2] S.K. Ratanathanawongs-Williams, In: *Field-Flow Fractionation Handbook*; M.E. Schimpf, K. Caldwell, J.C. Giddings, Eds. Wiley-Interscience, New York 2000; Chapter 17.
- [3] K.-G. Wahlund, In: *Field-Flow Fractionation Handbook*; M.E. Schimpf, K. Caldwell, J.C. Giddings, Eds. Wiley-Interscience, New York 2000; Chapter 18.
- [4] H.-L. Lee, J.F.G. Reis, J. Dohner, E.N. Lightfoot, *AIChE J.* **1974**, *20*, 776.
- [5] A. Carlshaf, J.A. Jönsson, *J. Chromatogr.* **1988**, *461*, 89.
- [6] J.A. Jönsson, A. Carlshaf, *Anal. Chem.* **1989**, *61*, 11.
- [7] J.A. Jönsson, A. Carlshaf, *J. Microcol. Sep.* **1991**, *3*, 411.
- [8] J. Granger, J. Dodds, *Sep. Sci. Technol.* **1992**, *27*, 1691
- [9] A. Carlshaf, J.A. Jönsson, *Sep. Sci. Technol.* **1993**, *28*, 1031.
- [10] A. Carlshaf, J.A. Jönsson, *Sep. Sci. Technol.* **1993**, *28*, 1191.
- [11] J.E.G.J. Wijnhoven, J.-P. Koorn, H. Poppe, W.Th. Kok, *J. Chromatogr. A* **1995**, *699*, 119.
- [12] J.E.G.J. Wijnhoven, J.-P. Koorn, H. Poppe, W.Th. Kok, *J. Chromatogr. A* **1996**, *732*, 307.
- [13] M. van Bruijnsvoort, W.Th. Kok, R. Tijssen, *Anal. Chem.* **2001**, *73*, 4736.
- [14] W.J. Lee, B.-R. Min, M.H. Moon, *Anal. Chem.* **1999**, *71*, 3446.
- [15] M.H. Moon, K.H. Lee, B.-R. Min, *J. Microcol. Sep.* **1999**, *11*, 676.

- [16] A. Lucas, F. Lepage, P. Cardot, In: *Field-Flow Fractionation Handbook*; M.E. Schimpf, K. Caldwell, J.C. Giddings, Eds. Wiley-Interscience, New York 2000; Chapter 29.
- [17] S. Saenton, H.K. Lee, Y. Gao, J. Ranville S.K. Ratanathanawongs Williams, *Sep. Sci. Technol.* **2000**, *35*, 1761.
- [18] T. Shimada, T. Sakazaki, *Jpn. J. Med. Sci. Biol.* **1977**, *30*, 275.
- [19] P. Reschiglian, D. Melucci, G. Torsi, *Chromatographia* **1997**, *44*, 172.
- [20] P. Reschiglian, A. Zatonni, D. Melucci, C. Locatelli, G. Torsi, *Recent Res. Devel. Appl. Spectr.*, S.G. Pandalai Ed., Research Signpost, 1999, Vol. 3 (2000), p. 61.
- [21] P. Reschiglian, A. Zatonni, D. Melucci, G. Torsi, *Rev. Anal. Chem.* **2001**, *20*, 239.
- [22] M.J. Groves, In: *Modern Methods of Particle Size Analysis*. H.G. Barth, Ed. Wiley-Interscience, Toronto 1984, Chapter 2, pp. 43–48.
- [23] B.B. Weiner, In: *Modern Methods of Particle Size Analysis*. H.G. Barth, Ed. Wiley-Interscience, Toronto 1984, Chapter 3, pp. 93–116.
- [24] K.D. Caldwell, Z.-Q. Cheng, P. Hradecky, J.C. Giddings, *Cell Biophysics* **1984**, *6*, 233.
- [25] N.E. Assidjo, T. Chianéa, I. Clarot, F. Dreyfuss, Ph.J.P. Cardot, *J. Chromatogr. Sci.* **1999**, *37*, 229.
- [26] K.-G. Wahlund, A. Zatonni, Abstracts of Papers, FFF 2001, 19<sup>th</sup> International Symposium on Field-Flow Fractionation, Golden, Colorado, USA, June 26–29, 2001; Abstract L1.
- [27] P. Reschiglian, A. Zatonni, B. Roda, S. Casolari, M.-H. Moon, J. Lee, K. Rodmalm, G. Cenacchi, *Anal. Chem.* submitted.
- [28] P. Reschiglian, D. Melucci, G. Torsi, *J. Chromatogr. A* **1996**, *740*, 245.
- [29] P. Reschiglian, D. Melucci, L. Malló, M. Hansen, A. Kummerow, M. Miller, *Anal. Chem.* **2000**, *72*, 5945.
- [30] A. Zatonni, E. Loli Piccolomini, P. Reschiglian, G. Torsi, Abstracts of Papers, FFF 2001, 19<sup>th</sup> International Symposium on Field-Flow Fractionation, Golden, Colorado, USA, June 26–29, 2001; Abstract L14.
- [31] B.R. Min, S.J. Kim, K.-H. Ahn, M.H. Moon, *J. Chromatogr. A* **2002**, *950*, 175.

[JSS 1128]